CHEMBIOCHEM

Supporting Information

A Synthetic Mirror Image of Kalata B1 Reveals that Cyclotide Activity Is Independent of a Protein Receptor

Lillian Sando,[a] Sónia Troeira Henriques,[a, b] Fiona Foley,[a] Shane M. Simonsen,[a] Norelle L. Daly,[a] Kristopher N. Hall,[c] Kirk R. Gustafson,[d] Marie-Isabel Aguilar,[c] and David J. Craik*[a]

cbic_201100450_sm_miscellaneous_information.pdf

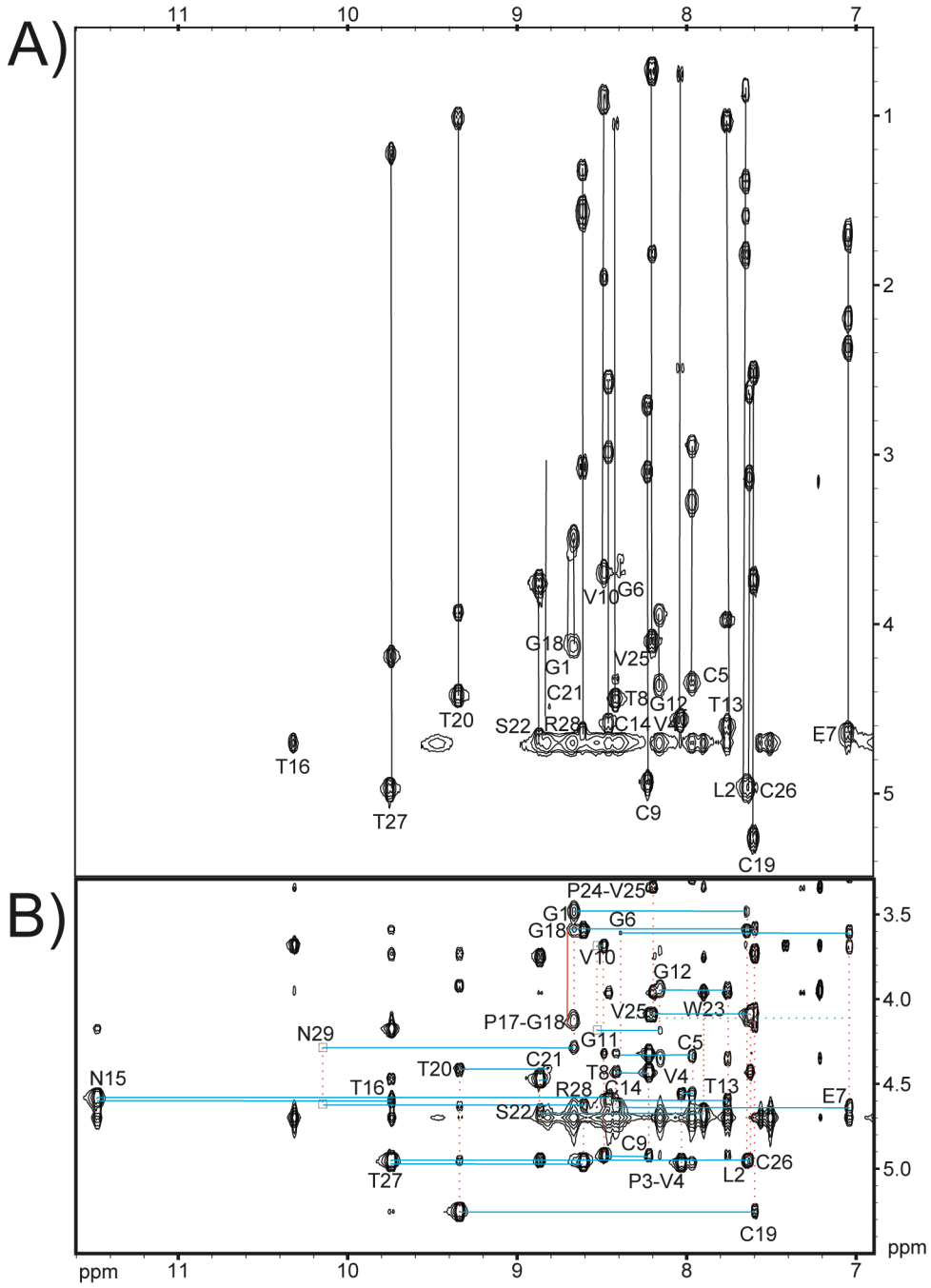

Figure S.1. Two-dimensional ^{1}H NMR spectra of D-kalata B1 (500 MHz, 298 K, pH 5.2, 95% H_2O / 5% D_2O). A) TOCSY spectrum with spin systems identified. Resonances for Gly11, Asn15 and Asn29 are absent from this display due to exchange broadening but were identified at lower pH. Trp23 was absent from the TOCSY spectra but could be identified by NOESY. B) Fingerprint region of NOESY spectrum with intra-residual Hα-HN crosspeaks labelled with residue numbers, red and blue lines corresponding to intra and inter-residual steps respectively illustrate the sequential walk, which is used to link the spin systems together during the assignment process. The sequential connectivity pattern is broken at the Pro residues, Gly^{11} and Asn^{29}. Crosspeaks for the latter two were observed in spectra recorded under other solution conditions and are indicated by boxes.

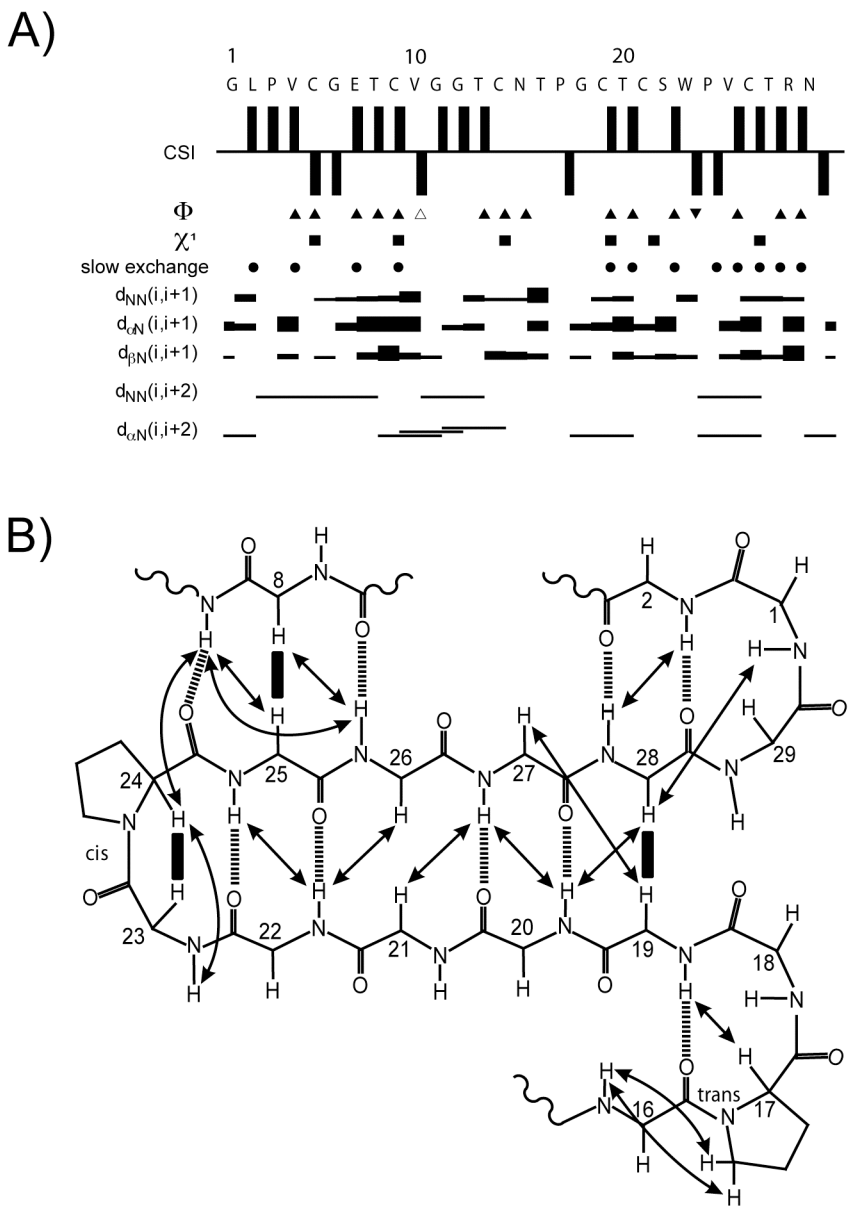

Figure S.2. Schematic representations of spectral data and secondary structure for D-kalata B1. A) Summary of the sequential and medium range NOE connectivities for D-kalata B1. The chemical shift index (CSI) for each residue is shown as a bar plot, with values of ± 1 indicating a shift deviation from random coil values of > 0.1 ppm, The $^{3}J_{HN\text{-}H_\alpha}$ coupling constants above 8 Hz and below 6 Hz are shown as filled triangles pointing upward or downward, respectively. The ϕ angle restraint of 100° ± 80° for Val^{10} is represented as an open triangle. Residues with χ_1 angle restraints are shown as filled bars, slowly exchanging amide protons as filled circles and sequential and medium-range NOEs shown with heights corresponding to the relative NOE intensities. B) Schematic diagram of the secondary structure of D-kalata B1 showing the inter-strand NOE (solid lines) and potential hydrogen bonds (dashed lines). Inter-residual HN-HN, Hα-HN and Hα-Hα NOEs are shown with arrows. For clarity, sequential NOEs are omitted. The α-carbon atoms are labelled according to their residue numbers. The peptide bonds between the proline residues and their preceding residues are denoted as either *cis* or *trans*. The hydrogen bonds were inferred from slow exchange data and preliminary structure calculations.

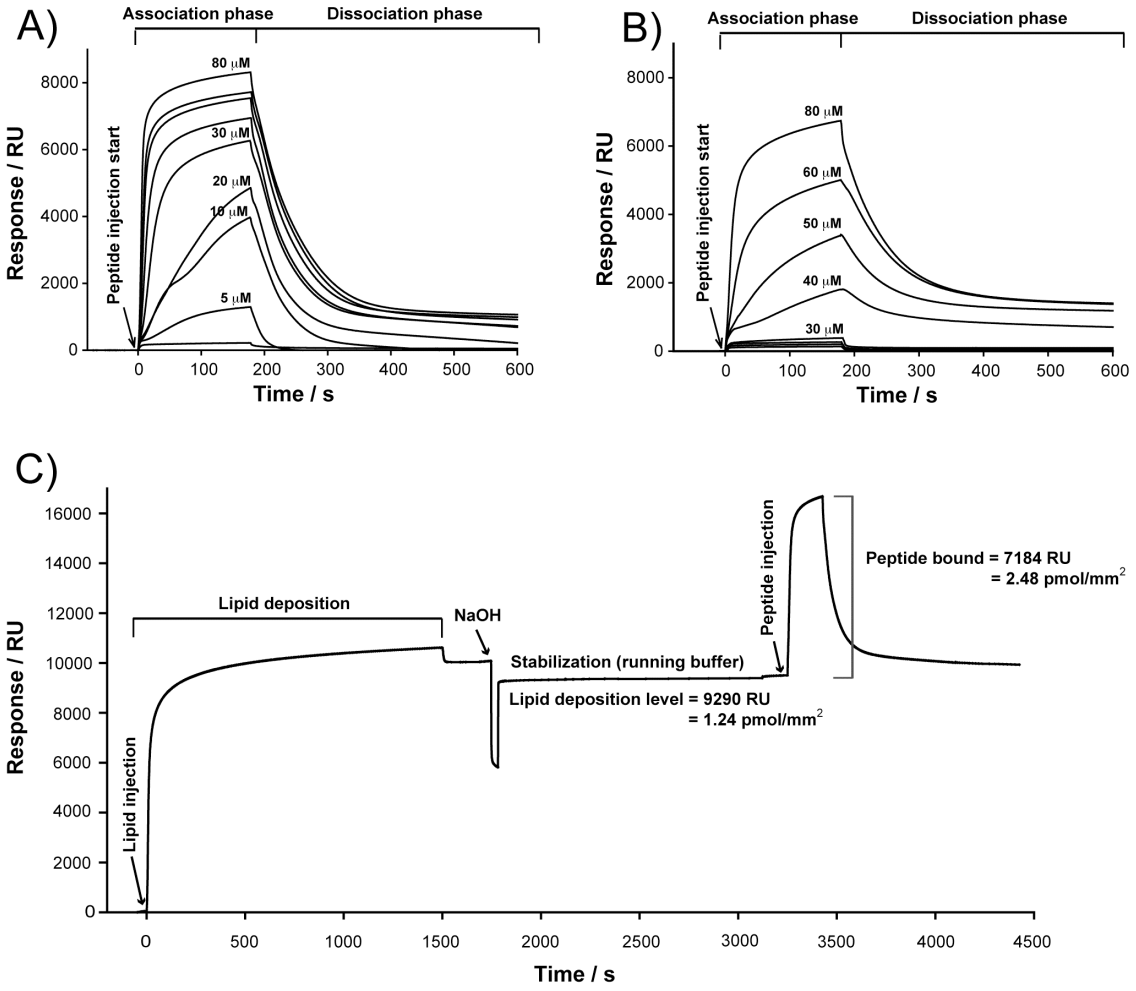

Figure S.3. Membrane binding of native kalata B1 and D-kalata B1 analysed by surface plasmon resonance. A) Native kalata B1 and B) D-kalata B1 were injected during 180 s (association phase) over POPC/POPE (4:1) lipid surfaces deposited on a L1 chip. Dissociation of the peptide from the membrane was followed for 600 s (dissociation phase). Different concentrations of peptide were injected (0, 5, 10, 20, 30, 40, 50, 60, 80 μM), and selected sensorgrams are labelled to assist with identification. C) Deposition of membrane vesicles composed of POPC/POPE (4:1) in the L1 chip (2 μL/min, 25 min). 20 mM NaOH solution was injected after the lipid deposition to remove loosely bound vesicles. The peptide was injected over the lipid surface during 180 s (here exemplified with 50 μM 75% L / 25% D-kalata B1 mixture) and peptide dissociation was followed for 600 s. Peptide/lipid ratio at the end of peptide association phase can be determined by converting the response units (RU) into moles of peptide and lipid (1 RU ~ 1pg/mm^2 of lipid or peptide). M_w POPC/POPE (4:1) ~ 752; M_w kalata B1 = 2892.33.

Table S.1. ^{1}H Chemical shifts (ppm) of D-kalata B1 at pH 5.2 and 298 K.

Residue	HN	Hα	Hβ	Others
Gly^{1}	8.667	4.14, 3.487	-	
Leu^{2}	7.649	4.962	1.812, 1.592	Hγ 1.384, Hδ_1* 0.881, Hδ_2* 0.808
Pro^{3}	-	4.964	2.353, 1.627	Hδ* 3.667, Hγ 2.054, 1.946
Val^{4}	8.035	4.559	2.486	Hγ_1* 0.774, Hγ_2* 0.73
Cys^{5}(I)	7.966	4.342	3.271, 2.94	
Gly^{6}	8.38	3.697, 3.606	-	
Glu^{7}	7.042	4.638	1.737, 1.675	Hγ 2.361, 2.188
Thr^{8}	8.418	4.435	4.32	Hγ_2* 1.035
Cys^{9}(II)	8.223	4.93	3.092, 2.701	
Val^{10}	8.486	3.689	1.958	Hγ_1* 0.927, Hγ_2* 0.861
Gly^{11}	8.549	4.187, 3.715	-	
Gly^{12}	8.157	4.359, 3.954	-	
Thr^{13}	7.758	4.602	3.972	Hγ_2* 1.024
Cys^{14}(III)	8.461	4.588	2.971, 2.558	
Asn^{15}	11.477	4.586	2.648, 2.648	Hδ_{21} 7.566, Hδ_{22} 6.755
Thr^{16}	9.741	4.177	3.733	Hγ_2* 1.213
Pro^{17}	-	4.141	2.212, 1.795	Hδ 4.108, 3.593, Hγ 2.033, 1.899
Gly^{18}	8.695	4.095, 3.592	-	
Cys^{19}(IV)	7.6	5.257	3.736, 2.512	
Thr^{20}	9.342	4.418	3.932	Hγ_2* 1.009
Cys^{21}(V)	8.818	4.474	2.979, 2.676	
Ser^{22}	8.866	4.667	3.753, 3.753	
Trp^{23}	7.898	3.965	3.148, 3.148	Hδ_1 7.214, Hε_1 10.315, Hε_3 7.318, Hη_2 7.115, Hζ_2 7.417, Hζ_3 7.005
Pro^{24}	-	3.346	1.591, -0.405	Hδ 3.095, 3.095, Hγ 1.233, 1.16
Val^{25}	8.2	4.089	1.816	Hγ_1* 0.765, Hγ_2* 0.716
Cys^{26}(VI)	7.626	4.948	3.127, 2.622	
Thr^{27}	9.742	4.963	3.589	Hγ_2* 0.766
Arg^{28}	8.612	4.641	1.607, 1.551	Hδ 3.093, 3.061, Hγ* 1.318
Asn^{29}	-	4.292	2.979, 2.735	Hδ_{21} 7.502, Hδ_{22} 6.857

Table S.2. NMR and refinement statistics for D-kalata B1

	Protein
NMR distance and dihedral restraints	
Distance constraints	
Total NOE	265
Intra-residue	0
Inter-residue	265
Sequential ($\|i - j\| = 1$)	109
Medium-range ($\|i - j\| \leq 4$)	56
Long-range ($\|i - j\| \geq 5$)	100
Intermolecular	0
Hydrogen bonds	10
Total dihedral angle restraints	
ϕ	15
χ_1	9
Structure statistics	
Violations (mean and s.d.)	
Distance restraints (Å)	0.038 ± 0.002
Dihedral angle restraints (º)	0.44 ± 0.13
Max. dihedral angle violation (º)	2.5
Max. distance restraint violation (Å)	0.3
Deviations from idealized geometry	
Bond lengths (Å)	0.005 ± 0.0002
Bond angles (º)	0.67 ± 0.03
Impropers (º)	0.67 ± 0.026
Average pairwise r.m.s. deviation** (Å)	
Backbone	0.36 ± 0.10
Heavy	0.94 ± 0.19

** Pairwise r.m.s. deviation was calculated among 20 refined structures.